ISSN: 2395-7639

International Journal of Multidisciplinary Research in Science, Engineering, Technology & Management (IJMRSETM)

(A Monthly, Peer Reviewed Online Journal)

Visit: www.ijmrsetm.com

Volume 4, Issue 10, October 2017

A Novel Multiband Multichannel Variational Approach Based on NLTV Model for Image Inpainting

Gaurav Chouhan[1]

Department of ECE, L.R.College of Engineering and Technology, Solan (H.P), India [1]

ABSTRACT: An increasingly popular area of research in the field of digital image processing is image inpainting where the removal of undesired objects and reconstruction of the missing or damaged parts of the digital images has become the fundamental problem. Image inpainting is the practice of solving these problems where the damaged or missing portions of the images are reconstructed in a visually plausible manner. In this paper, an effectual inpainting technique is presented for the removal of the unsought objects and reconstruction of the digital images. The basic idea behind this technique is to convert the multichannel image into multiple-bands (RGB) and then employ BOS and NLTV model for the optimization of proposed multiband-MNLTV model. The proposed model is tested over a number of digital images. The experimental results prove the multiband-MNLTV model a novel approach, in both its accuracy and contrast invariance.

KEYWORDS: Inpainting, multiband, multichannel nonlocal total variation (MNLTV), image restoration.

I. INTRODUCTION

The detection and removal of the degradation in digital images is fundamental in the restoration process. Image inpainting refers to the filling-in of regions of missing information and replacement of regions by using surrounding information. It has been widely investigated in the applications of image coding (reconstructing lost parts), digital effects (removal of undesirable objects) and image restoration (scratch or text removal in photograph) [1]. Image inpainting, a set of techniques for making undetectable modifications to images, is as ancient as art itself. The term inpainting comes from art restoration, where it is known as retouching. The need to retouch the image in an unobtrusive way extended naturally from paintings to photography and film. The word “inpainting” was initially invented by museum or art restoration workers [14] [15]. Image inpainting refers to the process of manipulating an image or a region of an image. An example of manual inpainting is shown in fig.1 in which the inpainting was done by an art restoration worker.

(a) Original image (b) Image after manual inpainting

Fig. 1: An example of image inpainting [16].

The concept of “digital inpainting” in image processing was introduced by Bertalmio et.al [17]. They developed the inpainting models based on higher order PDEs. In the digital domain, the inpainting problem was first appeared under the name “error concealment" in telecommunications, where the need was to fill-in image blocks that had been lost during data transmission. “Image disocclusion," was one of the first works to address inpainting since it treated the

ISSN: 2395-7639

International Journal of Multidisciplinary Research in Science, Engineering, Technology & Management (IJMRSETM)

(A Monthly, Peer Reviewed Online Journal)

Visit: www.ijmrsetm.com

Volume 4, Issue 10, October 2017

image gap as an occluding object that had to be removed, and the image underneath would be the restoration result. Popular terms used to denote inpainting algorithms are "image completion", "image fill-in" and "image retouching".

(a) A digitized scratched photograph (b) Image after inpainting
Fig.2: Restoration of an old photograph [17]

In this paper, a multiband-multichannel nonlocal total variation (multiband-MNLTV) model is proposed to solve the inpainting problem of digital images by making use of the NLTV model defined in [7] and [8]. In order to improve the implementation efficiency of the multiband-MNLTV model, a Bregmanized operator splitting algorithm, presented in [9] and [10], is employed.
The rest of this paper is organized as follows. In Section III, the multiband-MNLTV model is formulated. The parameters description and experimental results are presented in Section IV. Section V is the conclusion.

II. RELATED WORK

In order to solve the inpainting problem of the old paintings and digital images, a number of methods have been proposed. The first variational approach to the image inpainting problem was proposed by Nitzberg and Mumford [2]. They proposed a segmentation algorithm that finds the 2.1-D sketch of an intensity image in different stages. "Level lines based disocclusion", was another variational approach to the image inpainting problem suggested by Masnou and Morel [3]. A fast image inpainting algorithm based on total variation (TV) model was presented by Lu et.al [4]. Their model was basically a weighted-average algorithm which meant that, smaller the difference between the target-pixel and the neighbourhood-pixels, greater the weight on the contrast and vice-versa. The work in [5] described a nonlocal total variation (NLTV) image restoration model. NLTV model makes use of the more information than the classical TV model. Anisotropic filter is used in this approach to avoid the blurring effect of the Gaussian noise. The neighbourhood filtering which restores a pixel by taking an average of the values of neighbouring pixels is done in NLTV model. In [6], the authors presented a multichannel nonlocal total variation model for image inpainting. Their model takes advantages of nonlocal method which deals effectively with large-scale areas and textured images. MNLTV model is more robust than the NLTV model but this model is restricted to a single band.

III. PROPOSED ALGORITHM

The flow chart of the proposed multiband MNLTV model has been shown in Figure 3. The input image is the original image which has to be inpainted. After the input image read by the algorithm, the object which has to be removed is selected manually. Then the binary mask of the target object is fabricated. Now the input image is converted into multichannel image. The class multichannel is used to store color images where each color or band is stored as an independent grayscale image.

ISSN: 2395-7639

International Journal of Multidisciplinary Research in Science, Engineering, Technology & Management (IJMRSETM)

(A Monthly, Peer Reviewed Online Journal)

Visit: www.ijmrsetm.com

Volume 4, Issue 10, October 2017

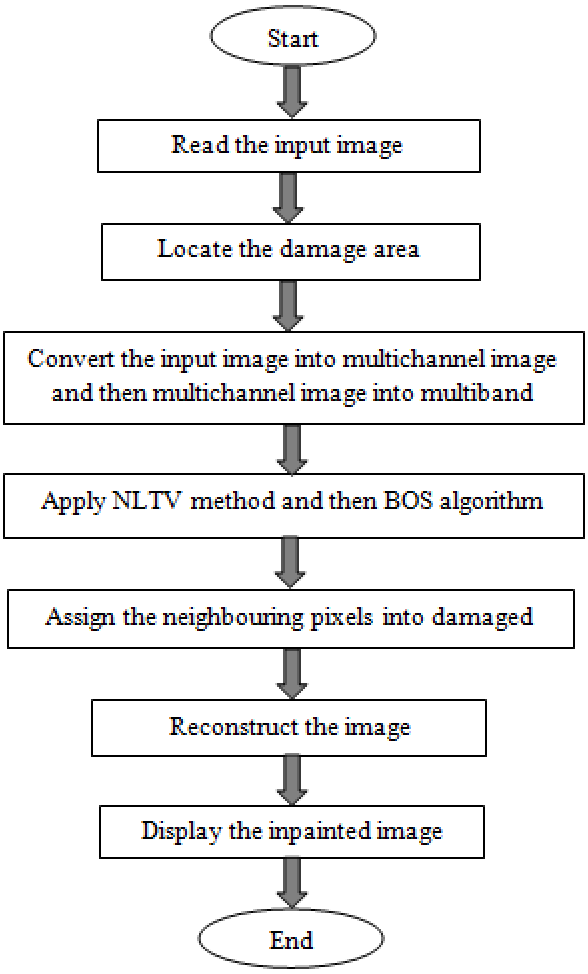

Fig.3: Flow Chart of the proposed model

This allows for each band in the image to be independently processed or modified easily. Then the multichannel image is converted into multiband image. A multi-spectral (multiband) image is a collection of several monochrome images of the same scene, each of them taken with a different sensor. Each image is referred to as a band. A well known multi-spectral or multi-band image is a RGB color image, consisting of a red, a green and a blue image. In the next step the NLTV and BOS algorithm is applied. After that the neighbouring pixels of the image are applied in the removed region. Then the inpainted image is reconstructed by the algorithm and displayed.

B. Description of the Proposed Algorithm:

Consider a digital image u with some missing pixels or undesirable object. The size of the image can be calculated as:

$$\frac{S = h \times w \times b \times dpi^2}{8} \qquad (1)$$

Where h is the height of the image, w is the width and b is the bit-depth of the image. Assume that the image u is of size $M \times N \times B$, where M is the samples of the image, N is the lines of the image and B is the number of bands.

Having a reference image f defined on Ω where Ω is its pixel domain, then the NL-means filtered image NLM_f [7] at point x will be:

$$NLM_f(u)(x) := \frac{1}{C(x)} \int_{\Omega} \omega_f(x,y)\, u(y) dy \qquad (2)$$

ISSN: 2395-7639

International Journal of Multidisciplinary Research in Science, Engineering, Technology & Management (IJMRSETM)

(A Monthly, Peer Reviewed Online Journal)

Visit: www.ijmrsetm.com

Volume 4, Issue 10, October 2017

The RGB images are often contaminated by Gaussian noise and can be restored by bilateral filters. In Bilateral filters, the intensity value of pixel *x* is replaced by a weighted average of the intensities of all other pixels. The weight function $\omega_f(x,y)$ depends upon the spatial distance between the central pixel and other pixels as well as on the difference of their intensities. Moreover, the weight function $w_f : \Omega \times \Omega$ is a non-negative and symmetric function which measure the similarity between any two pixels *x* and *y*.

$$w_f(x,y) = w_s(x,y) \cdot w_I(x,y) \tag{3}$$

where

$$w_s(x,y) = \exp\left(-\frac{\|x-y\|^2}{2\sigma_s^2}\right)$$
$$w_I(x,y) = \exp\left(-\frac{|I(x)-I(y)|^2}{2\sigma_I^2}\right)$$

Here $\|\cdot\|$ denotes the Euclidean distance between pixels *x* and *y*, σ_s and σ_I are the tuning parameters in the spatial and intensity domains respectively.

The weight function between two points *x* and *y* defined in equation 2 can be computed by using the difference of patches around each point.

$$C(x) := \int_\Omega w_f\,(x,y)\;dy \tag{4}$$

where $C(x,y)$ is a cost function of the minimum path connecting *x* and *y*. For the color images, the connection costs are calculated using Euclidean distance in RGB color space between neighbouring pixels. Due to the significance of the nonlocal operators in the proposed multiband-MNLTV model, the definitions of the nonlocal TV regularization functions introduced in [11] are given in the following. Let $\Omega \subset R^2$, $(x,y) \in \Omega$, $u : \Omega \to R$ be the given function defined on Ω to represent the pixel values of an image and $\omega_f(x,y)$ is a non-negative and symmetric weight function.

The nonlocal gradient $\nabla_w\, u(x) : \Omega \to \Omega \times \Omega$ for the points x and y in an image is defined as:

$$\nabla_w\, u\,(x,y) := (u(x) - u(y))\sqrt{w(x,y)}, \qquad \forall\, x,y\, \Omega \tag{5}$$

The nonlocal H^1 norm and NLTV can be defined as:

$$J^w_{NLH^1}(u) := \int_\Omega |\nabla_w\, u(x)|^2\, dx \;=\; \int_{\Omega\times\Omega} \big(u\,(x) - u(y)\big)^2 w(x,y)\, dx\, dy \tag{6}$$

$$J^w_{NLTV}(u) := \int_\Omega |\nabla_w\, u(x)|\, dx \;=\; \int_\Omega \sqrt{\int_\Omega (u(x) - u(y))^2\, w(x,y) dx dy} \tag{7}$$

IV. SIMULATION RESULTS

In this section, we have presented two experiments to demonstrate the efficiency of the multiband-MNLTV model. In order to verify the performance of the multiband-MNLTV model, different image quality evaluation methods are determined which work for various kinds of image degradations. Furthermore they are compared with the existing image inpainting model presented in [6].

PSNR is used as a criterion for the quality of the restoration which is usually expressed in terms of the logarithmic decibel scale. Higher the value of PSNR, better the quality of the reconstructed image whereas a small value of the PSNR implies the high numerical differences between images. Another well-known quality metric SSIM [12] is used to measure the similarity between two images. Structural similarity index metric measure the image quality based on initial uncompressed data. In order to give a quantitative assessment of the inpainting result from a human vision aspect, the metric Q index [13] is used.

ISSN: 2395-7639

International Journal of Multidisciplinary Research in Science, Engineering, Technology & Management (IJMRSETM)

(A Monthly, Peer Reviewed Online Journal)

Visit: www.ijmrsetm.com

Volume 4, Issue 10, October 2017

(a) (b) (c)

Fig.4: Experimental results for the recovery of background data.

Fig. 4(a) shows the original image to be inpainted. Fig. 4(b) is the result of MNLTV algorithm and fig.4(c) is the result of multiband-MNLTV algorithm.

The first simulated data test of the multiband-MNLTV algorithm is for the recovery of background data in a digital image. Fig.4(a) shows the original digital image. In this experiment, the simulated image consist of a bunjee jumper which is removed by multiband-MNLTV algorithm. Fig.4(c) shows that the output of proposed multiband-MNLTV algorithm is better than the output of MNLTV model shown in Fig.4(b). We also simulate the aditive noise by adding different variance of Gaussian noise in different bands shown in Table1(a).

Parameter	Standard Deviation	MNLTV Model	Multiband MNLTV
PSNR (db)	1	30.947	31.991
	2	30.943	32.241
	3	30.929	32.285
	4	30.935	32.195
	5	30.936	32.087
	6	30.701	32.183
	7	30.880	32.570

(a)

Parameter	MNLTV Model	Multiband MNLTV
SSIM	0.9663	0.9803
Q	0.5396	0.7452

(b)

Table 1: PSNR, SSIM and Q-Metric values for the first experiment.

Table 1(a) shows the PSNR values corresponding to different values of σ for the simulated experimental result and table 1(b) shows the SSIM and Q-index values for the given input image.

Second simulation experiment involves the removal of mainstay of the bridge.

ISSN: 2395-7639

International Journal of Multidisciplinary Research in Science, Engineering, Technology & Management (IJMRSETM)

(A Monthly, Peer Reviewed Online Journal)

Visit: www.ijmrsetm.com

Volume 4, Issue 10, October 2017

(a) (b) (c)

Fig.5: Experimental results for the removal of mainstay of the bridge.

Fig. 5(a) shows the original input image. Fig. 5(b) and 5(c) shows the output results of the MNLTV and multiband-MNLTV model respectively.

Parameter	Standard Deviation	MNLTV Model	Multiband MNLTV
PSNR (db)	2	15.947	17.316
	4	15.990	17.522
	6	16.067	17.200
	8	16.254	17.361
	10	16.602	17.067
	12	15.857	17.517
	14	16.051	17.102

(a)

Parameter	MNLTV Model	Multiband MNLTV
SSIM	0.9983	0.9992
Q	0.9838	0.9924

(b)

Table 2: PSNR, SSIM and Q-Metric values for the input image II.

Table 2(a) shows the PSNR values corresponding to different values of σ for the simulated experimental result and table 2(b) shows the SSIM and Q-index values for the given input image.

The third simulated experiment is carried out for the removal of a carry bag shown in figure 6(a).

(a) (b) (c)

Fig.6: Experimental results for removing object using Image Inpainting.

Fig.6(a) shows the original input image consisting of the undesired object. The outputs of the MNLTV and multiband-MNLTV model are shown in fig.6(b) and 6(c) respectively.

ISSN(Online): 2320-9801
ISSN (Print): 2320-9798

International Journal of Innovative Research in Computer and Communication Engineering

(An ISO 3297: 2007 Certified Organization)

Website: www.ijircce.com

Vol. 5, Issue 5, May 2017

Parameter	Standard Deviation	MNLTV Model	Multiband MNLTV
PSNR (db)	1	22.818	23.724
	2	22.061	23.761
	3	22.622	23.762
	4	22.857	23.199
	5	22.562	23.280
	6	22.778	23.394
	7	22.405	23.257

(a)

Parameter	MNLTV Model	Multiband MNLTV
SSIM	0.9958	0.9968
Q	0.9581	0.9675

(b)

Table 3: PSNR, SSIM and Q-Metric values for the input image II. (a) PSNR values corresponding to different values of σ for the simulated experimental result. (b) SSIM and Q-index values for the given input image.

GRAPHICAL REPRESENTATION OF PARAMTERS CALCULATED FOR THE ALL DATASET IMAGES:

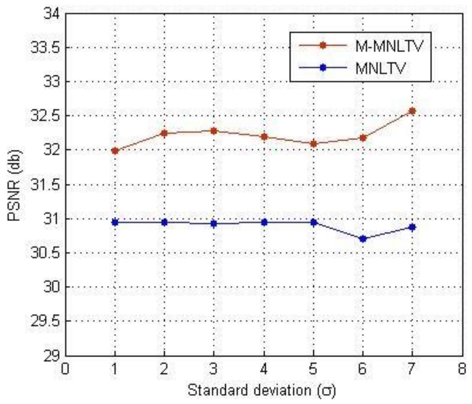

(a)

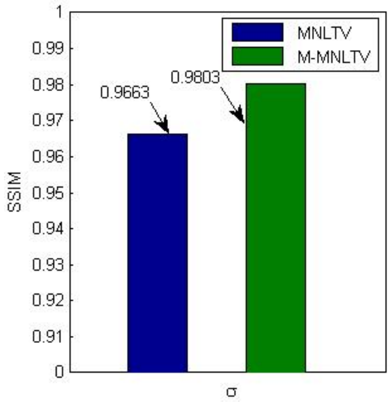

(b)

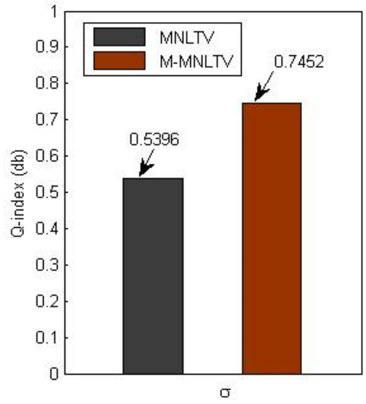

(c)

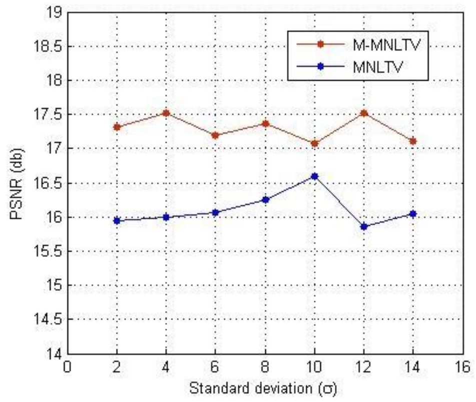

(d)

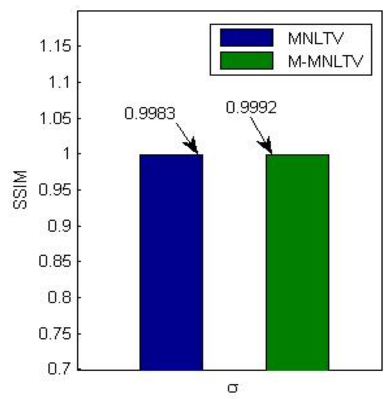

(e)

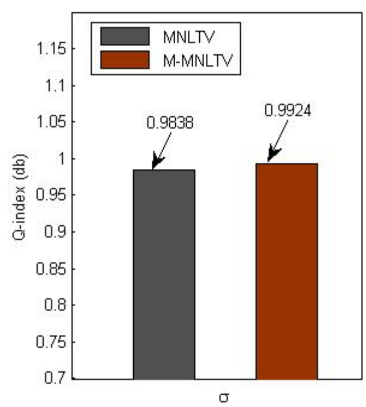

(f)

ISSN(Online): 2320-9801
ISSN (Print): 2320-9798

International Journal of Innovative Research in Computer and Communication Engineering

(An ISO 3297: 2007 Certified Organization)

Website: www.ijircce.com

Vol. 5, Issue 5, May 2017

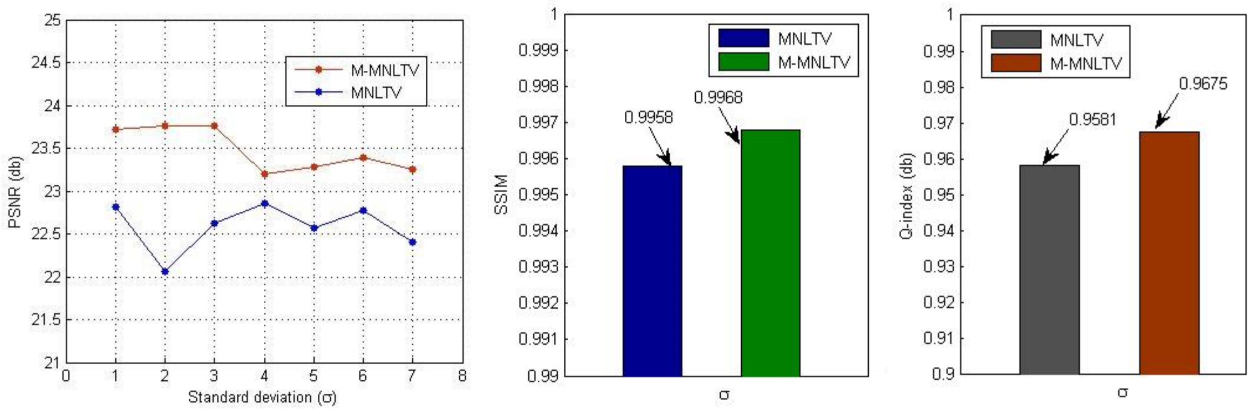

(g) (h) (i)

Fig.7: Graphical representation of PSNR, SSIM and Q-index values.

Fig. 7(a), (d), (g) represents the PSNR values corresponding to the different values of σ for the first, second and third simulated experimental results respectively. Fig. 7(b), (e), (h) represents the values of SSIM index for the first, second and third simulated experimental results respectively. Fig. 7(c), (f), (i) represents the values of Quality- index for the first, second and third simulated experimental results respectively.

V. Conclusion and Future Work

In this paper, a multiband-MNLTV model has been presented to deal with the fundamental problems of image inpainting. The proposed multiband-MNLTV model is applied to remove the bunjee jumper, the mainstay of the bridge and a carry bag from the digital input images. The parametric study for the first simulated experiment showed that the average PSNR value of multiband-MNLTV model is 32.221 db, whereas for MNLTV model, the average PSNR value is 30.895 db. Similarly, for second simulated experiment, the average PSNR for multiband-MNLTV model and existing MNLTV model are 17.297 db and 16.109 db respectively. For third simulated experiment, the average PSNR for multiband-MNLTV model and existing MNLTV model are 23.482 db and 22.586 db respectively. Both the models are tested over a dataset of ten images. The maximum percentage increase in PSNR for multiband-MNLTV model over MNLTV model is 8.73% and the minimum increase is 1.28%. The SSIM and Q-index results are also better for multiband-MNLTV model. Hence from these simulated data experiments, it is concluded that the restoration results using proposed multiband-MNLTV algorithm are much better than the existing image inpainting model. Although the proposed multiband-MNLTV model is more robust than the existing MNLTV model, still it is restricted only to the digital images. It does not work for the object removal form the digital videos. So in the near future, the present work can be extended or will be helpful in video inpainting.

REFERENCES

1. Z. Xu and J. Sun, “Image inpainting by patch propagation using patch sparsity”, IEEE Transactions on Image Processing, vol. 19, no. 5, pp. 1153-1165, May 2010.
2. M. Nitzberg and D. Mumford, “The 2.1-D Sketch”, In Proceedings of 3rd International Conference on Computer Vision, pp. 138-144, Dec. 1990.
3. S. Masnou and J.M. Morel, “Level lines based disocclusion”, In Proceedings of International Conference on Image Processing, Chicago, vol. 3, pp. 259-263, 1998.
4. X. Lu, W. Wang and D. Zhuoma, “A fast image inpainting algorithm based on TV model”, Proc. of International Multi Conference of Engineers and Computer Scientists, Hong Kong, vol. 2, March 2010.
5. H. Chang, X. Zhang, X. C. Tai and D. Yang, “Domain decomposition methods for nonlocal total variation image restoration”, Springer, pp. 79-100, 2014.

6. Q. Cheng, H. Shen, L. Zhang and P. Li, "Inpainting for remotely sensed images with a multichannel nonlocal total variation model (MNLTV)", IEEE Transactions on Geoscience and Remote Sensing, vol. 52, no. 1, pp. 175-187, Jan. 2014.
7. A. Buades, B. Coll and J. M. Morel, "A review of image denoising algorithms with a new one", SIAM Journal for Multiscale Modelling and Simulation, vol. 4, no. 2, pp. 490-530, 2005.
8. A. Buades, B. Coll and J. M. Morel, "A non-local algorithm for image denoising", IEEE Conference on Computer Vision, vol. 2, pp. 60-65, June 2005.
9. X. Zhang, M. Burger, X. Bresson and S. Osher, "Bregmanized nonlocal regularization for deconvolution and sparse reconstruction", SIAM Journal for Imaging Sciences, vol. 3, no. 3, pp. 253-276, July 2009.
10. S. Osher, M. Burger, D. Goldfarb, J. Xu and W. Yin, "An iterative regularization method for total variation-based image restoration", Multiscale Modelling and Simulation, vol. 4, no. 2, pp. 460-489, June 2005.
11. G. Gilboa and S. Osher, "Nonlocal operators with applications to image processing", SIAM Journal on Applied Mathematics, vol. 7, no. 3, pp. 1005-1028, 2008.
12. Z. Wang, A. C. Bovik, H. R. Sheikh and E. P. Simoncelli, "Image quality assessment: From error visibility to structural similarity", IEEE Transactions on Image Processing, vol. 13, no. 4, pp. 1-14, April 2004.
13. X. Zhu and P. Milanfar, "Automatic parameter selection for denoising algorithms using a no-reference measure of image content", IEEE Transactions on Image Processing, vol. 19, no. 12, pp. 3116-3132, Dec. 2010.
14. S. Walden, "The Ravished Image", St. Martin's Press, New York, 1985.
15. G.Emile, "The Restore's Handbook of Easel Painting", Van Nostrand Reinhold, New York, 1976.
16. G. Sapiro, "Geometric partial differential equations and image analysis", Cambridge University Press, 2001.
17. M. Bertalmio, G. Sapiro, V. Caselles and C. Ballester, "Image Inpainting", In - Proceedings of ACM SIGGRAPH 27th annual Conference on Computer Graphics and interactive techniques, New Orleans, LA, pp. 417-424, 2000.